INTERMOLECULAR INTERACTIONS OF SAXAGLIPTIN AND VILDAGLIPTIN WITH HUMAN SERUM ALBUMIN**

S. Barghash [1], S. Abd El-Razeq [1], H. Elmansi [2*], M. A. Elmorsy [2], F. Belal [2]

[1] Analytical Chemistry Department, Faculty of Pharmacy (Girls), Al-Azhar University, Cairo, Egypt
[2] Faculty of Pharmacy, Mansoura University, Mansoura, 35516, Egypt; e-mail: dr_heba85@hotmail.com

The binding interactions between human serum albumin (HSA) and two anti-diabetic drugs, saxagliptin (SXG) and vildagliptin (VDG), are studied. Different approaches are adopted, including native fluorescence, synchronous fluorescence, UV–Visible absorption, and Fourier-transform infrared (FTIR) analysis, in addition to molecular docking simulations. Moreover, the thermodynamic parameters of the interactions are determined at different temperatures. The obtained results indicate that the intrinsic fluorescence of HSA is quenched via a static mechanism. Values for the binding constant, K_a, are 4.0×10^4, 2.49×10^4, and 2.42×10^4 L/mol for SXG, and 1.13×10^4, 8.54×10^3, and 7.15×10^3 L/mol for VDG at 298, 310, and 318 K, respectively. Evidence from competition experiments with site markers indicate that both SXG and VDG bind HSA primarily at or near site I of the protein. FTIR spectroscopy data indicate an alteration of the protein conformation in the presence of SXG or VDG. Indeed, the results of different spectroscopic analyses indicated that noticeable changes in the protein structure conformation occur following the addition of SXG or VDG.

Keywords: *human serum albumin, saxagliptin, vildagliptin, spectroscopy, protein binding constants.*

МЕЖМОЛЕКУЛЯРНЫЕ ВЗАИМОДЕЙСТВИЯ САКСАГЛИПТИНА И ВИЛДАГЛИПТИНА С СЫВОРОТОЧНЫМ АЛЬБУМИНОМ ЧЕЛОВЕКА

S. Barghash [1], S. Abd El-Razeq [1], H. Elmansi [2*], M. A. Elmorsy [2], F. Belal [2]

УДК 543.42:547.962.3

[1] Университет Аль-Азхар, Каир, Египет
[2] Университет Мансуры, Мансура, 35516, Египет; e-mail: dr_heba85@hotmail.com

(Поступила 8 сентября 2020)

Изучены связывающие взаимодействия между сывороточным альбумином человека (HSA) и двумя антидиабетическими препаратами — саксаглиптином (SXG) и вилдаглиптином (VDG). Использованы различные подходы, включая естественную флуоресценцию, синхронную флуоресценцию, спектроскопию поглощения УФ-видимого диапазона, ИК-Фурье-спектроскопию (FTIR), в дополнение к моделированию стыковки молекул. При разных температурах определены термодинамические параметры взаимодействий. Показано, что собственная флуоресценция HSA подавляется по статическому механизму. Получены константы связывания $K_a = 4.0\times10^4$, 2.49×10^4 и 2.42×10^4 л/моль для SXG и 1.13×10^4, 8.54×10^3 и 7.15×10^3 л/моль для VDG при 298, 310 и 318 K соответственно. Данные сравнительного эксперимента с индикаторами места связывания показывают, что SXG и VDG связывают HSA в основном в положении I белка или рядом с ним. Согласно результатам FTIR-спектроскопии, конформация белка изменяется в присутствии SXG или VDG. Результаты спектроскопического анализа свидетельствуют о том, что заметные изменения в конформации структуры белка происходят после добавления SXG или VDG.

Ключевые слова: *сывороточный альбумин человека, саксаглиптин, вилдаглиптин, спектроскопия, константы связывания с белками.*

**Full text is published in JAS V. 88, No. 6 (http://springer.com/journal/10812) and in electronic version of ZhPS V. 88, No. 6 (http://www.elibrary.ru/title_about.asp?id=7318; sales@elibrary.ru).

Introduction. Drugs can generally act on biological membranes as well as inside the cells, which are enclosed by membranes. Even in the latter situation, drugs must interact with membranes to cross them and reach their targets [1]. Therefore, the type and extent of these interactions have a direct effect on the pharmacological action of the drug, its biosafety, delivery time, and therapeutic efficacy. Drug molecules in the blood circulation are either bound to plasma proteins or present in the unbound (free) form. Bound drugs interact with human serum albumin (HSA) at two different binding sites, and examining the interactions between drug molecules and protein helps in the investigation of the crucial characteristics of the effect of drugs on the biological systems [2–4]. The data obtained from these interactions can give useful information on the reorganization of the absorption and circulation of drugs in the blood.

Diabetes is a chronic disease that alters the way the human body handles glucose in the blood [5, 6]. A relatively new group of oral anti-diabetic agents called dipeptidyl peptidase-4 (DPP-4) inhibitors exists, which perform their pharmacological activity by increasing the levels of glucagon-like peptide-1 (GLP-1) in blood circulation [7]. Notably, GLP-1 is released after meals, but it undergoes rapid degradation by DPP-4. Inhibitors of DPP-4, however, rapidly block the degradation of GLP-1, thus improving glycemic control [8]. DPP-4 inhibitors such as saxagliptin (SXG) and vildagliptin (VDG) (Fig. 1) are widely used, and they have been shown to be superior to traditional oral hypoglycemic agents in terms of efficacy and tolerability [9, 10]. SXG and VDG act by inhibiting the degradation of endogenous GLP-1 and glucose-dependent insulinotropic peptides [11]. Additionally, evidence suggests that, in patients, these drugs may improve diabetes-induced symptoms like learning and memory deficits [12]. The nature of the binding between SXG and VDG and HSA is expected to have a significant influence on the pharmacokinetics of the mentioned drugs.

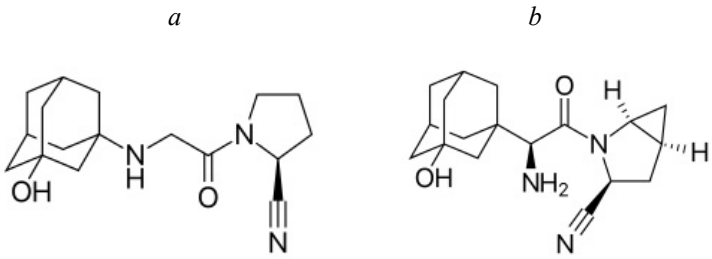

Fig. 1. Molecular model of (a) saxagliptin and (b) vildagliptin.

To our knowledge, the thermodynamics of the binding of SXG and VDG to HSA has not been reported in the literature. Hence, this study aims to acquire information about the binding by characterizing the interaction mode, calculating the binding constants (K_a), and locating the binding sites on HSA. Different spectroscopic methodologies were applied, including native fluorescence, synchronous fluorescence, UV-visible absorption, and Fourier-transform infrared (FTIR). In addition, a molecular docking approach was implemented.

Experimental. SXG certified to have 99.8% purity was provided by Bristol-Myers Squibb/Astra Zeneca EEIG (New Cairo, Cairo, Egypt). VDG certified to have 99.6% purity was provided by Novartis Company, EL Amiria, Cairo, Egypt. Diazepam (DIA) was provided by Amoun Pharmaceutical Co. (Cairo, Egypt). Indomethacin (IND) was obtained from Medical Union Pharmaceuticals (Ismailia, Egypt). TRIS (hydroxymethyl) aminomethane hydrochloride (TRIS–HCl) was of analytical reagent grade and obtained from Sigma Aldrich Co. (Heliopolis Cairo, Egypt). HSA was purchased from Sigma Aldrich Co. (Chemie Gmbh, Munich, Germany). Other supplementary chemicals were of analytical reagent grade. Double-distilled water was utilized during the study. An HSA (20.0 μM) stock solution was freshly prepared in distilled water. Stock solutions of SXG, VDG, and IND (100.0 μM) were also prepared fresh in distilled water. A stock solution of DIA (100.0 μM) was prepared in 50% aqueous methanol. A tris-HCl buffer solution at a concentration of 20.0 mM (pH 7.4) was prepared in distilled water. All the solutions were stored in a refrigerator at 4°C. A Cary Eclipse fluorescence spectrophotometer equipped with a Xenon flash lamp manufactured by Agilent Technologies (Germany) was used. The high voltage mode was used (800 V), and the slit width was 5 nm. The Shimadzu (Kyoto, Japan) UV-1601 PC, UV-Visible double-beam spectrophotometer was operated at a fast scan speed. A Hanna pH-meter (Romania) was used to allow the pH of the solutions to be adjusted.

FT-IR spectra were acquired on a Thermo Fisher Scientific Nicolet-iS10 FT-IR Spectrometer manufactured by Thermo Fisher Scientific (168 Third Avenue Waltham, MA USA).

Molecular modeling was carried out employing the Molecular Operating Environment software (MOE) [13]. MOE is a drug-discovery software platform that integrates visualization, modeling, and simulations. Both drugs were built and energy-minimized; they were then subjected to docking simulation to the protein obtained for the protein data bank (www.rcsb.org) representing HSA (pdb code: 1E7I). The receptor was kept rigid, the triangle matcher technique was then implemented for the placement phase, and the London *dG* function was used for scoring using 50 runs for each compound.

Measurements. *Fluorescence.* Aliquots from the stock solution of each drug were quantitatively transferred into 10-mL volumetric flasks to obtain solutions at a concentration ranging from 1.0 to 6.0 μM for each drug; subsequently, 1.0 mL of TRIS buffer (pH 7.4) and 1.0 mL of 20.0 μM HSA solution were added in succession, and the various solutions were brought to the desired final volumes using distilled water. The solutions were mixed up and maintained for 45 min at different temperatures (i.e., 298, 310, and 318 K). The fluorescence emission spectra were then recorded between 290 and 450 nm, and the fluorescence intensity was recorded at 338 nm after excitation at 280 nm. Competitive binding experiments were conducted using two site markers that are specific for the two principal binding sites of HSA: IND, specific for site I, and DIA, specific for site II [14]. These experiments were conducted using a constant concentration of HSA and a molecular ratio of 1:1 between HSA and the site marker; the concentration of each drug was instead made to vary up to a maximum value for the drug-to-protein ratio of 10. The fluorescence emission spectra were then recorded.

UV-Visible. The same procedure described to perform the fluorescence measurements was implemented to perform UV-Visible spectroscopy measurements using 5.0 mL of 20-μM HSA solution that also included the drugs being investigated at a concentration ranging from 10.0 to 60.0 μM. The measurements were conducted in parallel with blank solutions lacking the drug. The UV-visible absorption spectra were recorded in the 200–350 nm wavelength range at three different temperatures: 298, 310, and 318 K.

Synchronous fluorescence. Two different Δλ values were used to measure the synchronous fluorescence spectra (i.e., 60 and 15 nm), under imitated physiological conditions over the 225–550 nm wavelength range. A solution of HSA (2.0 μM) was added to different solutions of the two drugs ranging in the concentration range between 1.0 and 6.0 μM, and the synchronous spectra were then recorded.

FTIR. The FTIR spectra of HSA (200 μM) in the presence of TRIS buffer and in the absence and presence of SXG or VDG were recorded from 1550 to 1750 cm^{-1}.

Results and discussion. *Fluorescence quenching of HSA with SXG and VDG.* One of the most convenient methodologies to study the drug–protein binding process is fluorescence quenching [15]. SXG and VDG display no native fluorescence at the wavelength at which HSA does, so neither drug is expected to interfere with HSA fluorescence measurements. In Fig. 2 the fluorescence spectra of HSA are reported before and after its interaction with increasing concentrations of SXG or VDG. The fluorescence intensity was observed to decrease as the concentration of SXG or VDG increased, while the λ emission wavelength was observed to shift slightly. This indicates that, as a result of interactions between HSA and SXG or VDG, a certain alteration occurred in the microenvironment of the fluorophore of HSA (Trp213) [16].

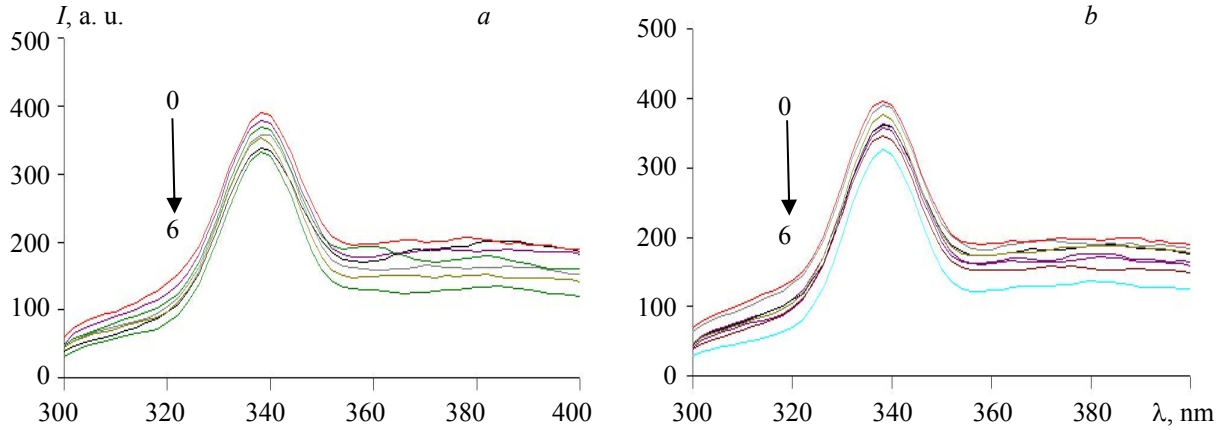

Fig. 2. Fluorescence spectra of HSA alone (2.0 μM) and in the presence of SXG and VDG: a) HSA-SXG complexes; b) HSA-VDG complexes excited at 280 nm at 298 K; concentrations 0, 1, 2, 3, 4, 5, and 6 μM.

UV-Visible absorption spectra of HSA with SXG and VDG. Given the simplicity of the use of UV-visible spectrometers, as well as their low cost and wide availability, UV-Visible spectroscopy can be used to investigate the basic alterations in protein besides examining the drug–protein complex formation [17]. HSA exhibits absorption bands in the 200–350 nm wavelength range that are related to its aromatic residues, such as tyrosine, tryptophan, and phenylalanine [18]. In this work, the characteristics of the UV-visible spectra were indicative of the formation of HSA-SXG and HSA-VDG complexes. Notably, the absorption spectra of the HSA solutions were recorded after increasing amounts of each of the studied drugs had been added to them. Two absorption bands due to HSA were observed after the interaction of this protein with each of the two drugs: a strong band at 210 (Fig. 3a,c) and a weak band at 280 nm (Fig. 3b,d). Increasing absorbance values for these bands were observed as the drug concentrations increased. This trend is due to the attainment of more extended conformation by the peptide back bone upon ligand binding in HSA. Notably, a slight bathochromic shift of the mentioned peaks was also observed. The results of this study suggest that the interaction between each of the two drugs and protein caused an alteration in the microenvironment in the albumin region; consequently, a certain change in hydrophobicity takes place [19, 20].

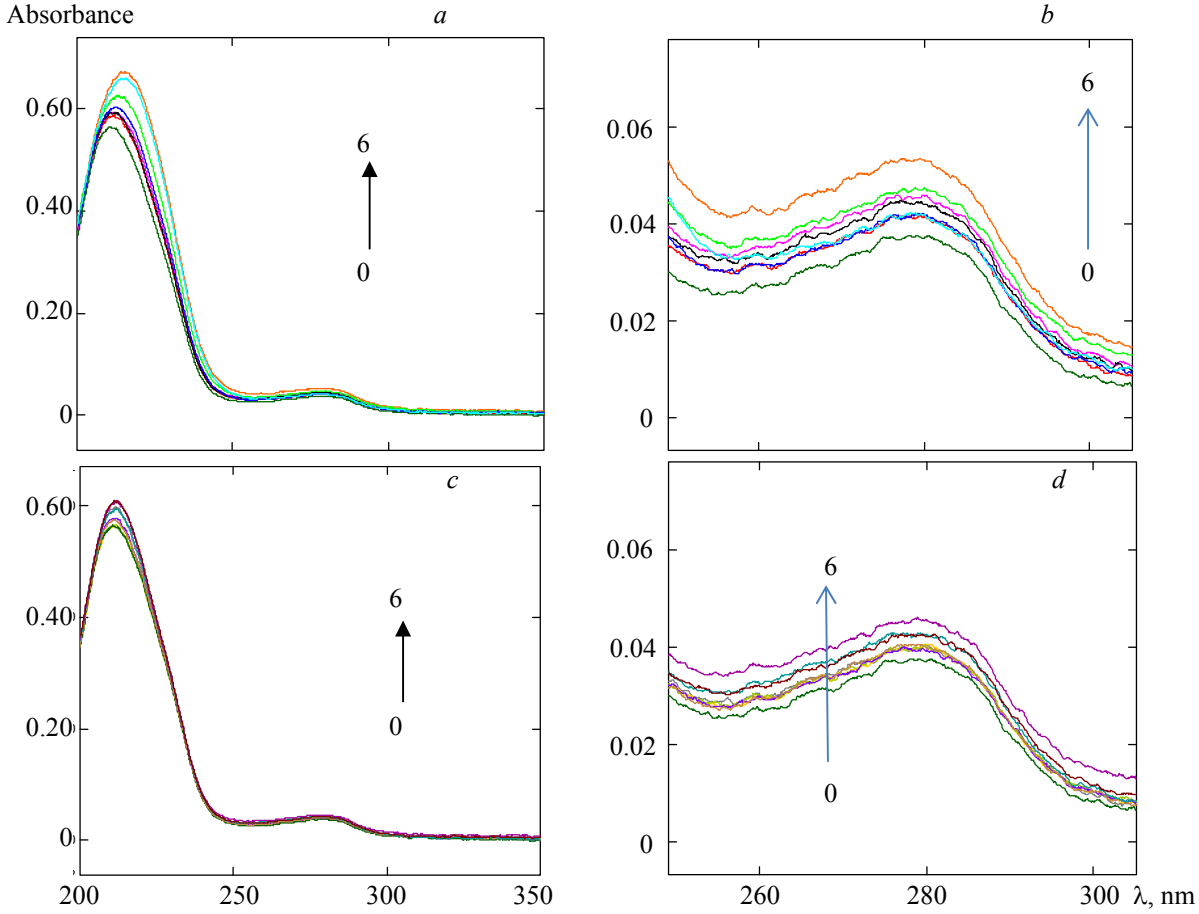

Fig. 3. UV spectra of HSA in the presence of a) saxagliptin at 210 nm, b) saxagliptin at 280 nm, c) vildagliptin at 210 nm, and d) vildagliptin at 280 nm; concentrations 0, 10, 20, 30, 40, 50, and 60 μM.

Synchronous fluorescence spectroscopy. Synchronous fluorescence spectroscopy (SFS) offers several advantages over fluorescence spectroscopy, including spectral bandwidth reduction and spectral simplicity [21]; therefore, SFS may provide data that illustrate the changes in the molecular environment of HSA, such as those experienced by the tyrosine or tryptophan residues after the drugs bind to HSA. SFS analysis focusing on the bands of tyrosine ($\Delta\lambda$ = 15 nm) and tryptophan ($\Delta\lambda$ = 60 nm) was employed to investigate the structural variations that occur in HSA upon it being exposed to different concentrations of SXG and VDG. The emission peaks of the tryptophan residues ($\Delta\lambda$ = 60 nm) showed a slight shift after the reaction with the two drugs (Fig. 4). This indicates that tryptophan residues undergo conformational changes because

the hydrophobicity decreases and the polarity increases [22]. This finding provided further proof that certain conformational alterations occur in HSA in the presence of SXG or VDG.

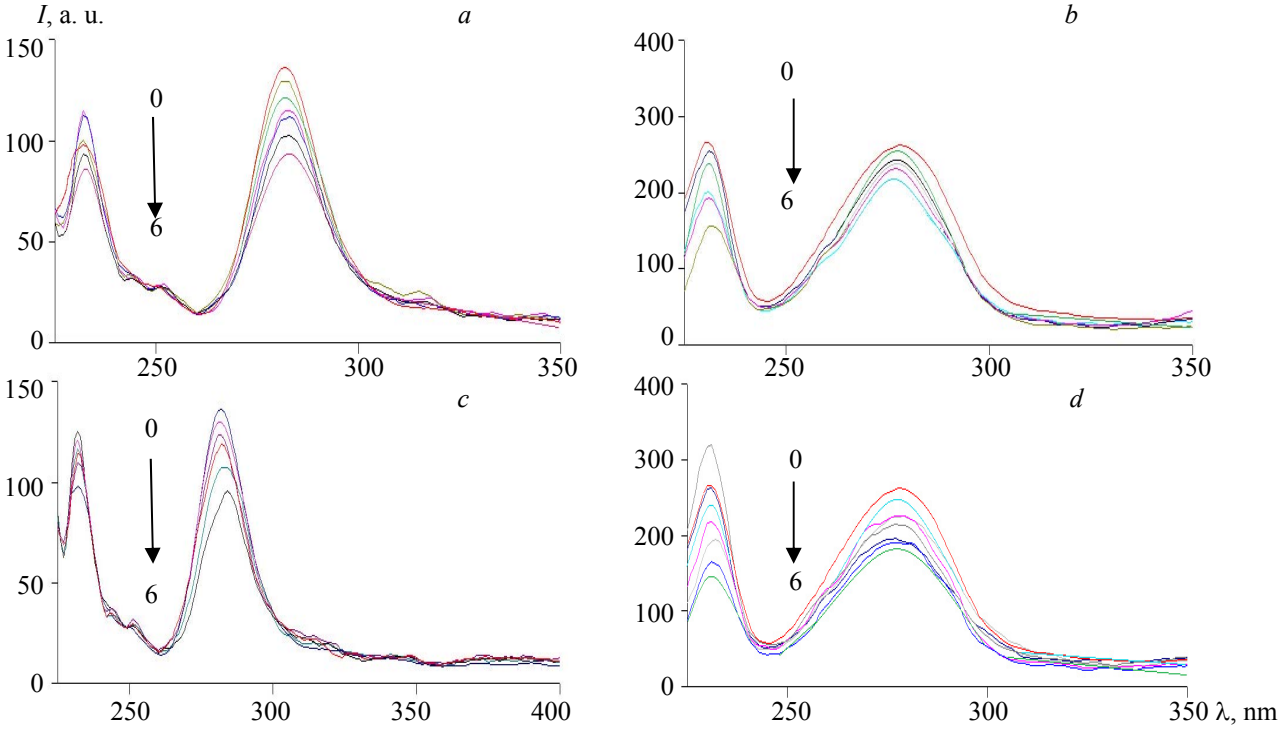

Fig. 4. Synchronous fluorescence spectra of HAS alone and in presence of SXG and VDG: a) HSA-SXG complexes at Δλ = 15 nm; b) HSA-SXG complexes at Δλ = 60 nm; c) HSA-VDG complexes at Δλ = 15 nm; d) HSA-VDG complexes at Δλ = 60 nm.

Mechanism of fluorescence quenching and result interpretation. The mechanism by which fluorescence is quenched can be classified as either dynamic or static. Ligand–albumin complexes are generally non-fluorescent in the case of static quenching; in dynamic quenching, on the other hand, the collisions result in fluorescent complexes. As the temperature increases, the dynamic quenching constant increases. That trend is attributed to the increase in value of the diffusion coefficients. By contrast, in static quenching, the quenching constant decreases in value in association with increases in temperature because of the instability of ground state complex. Notably, the Stern–Volmer equation illustrates the mechanism of fluorescence quenching [16]:

$$F/F^0 = 1 + K_{SV}[Q],$$

where F and F^0 represent the values for the fluorescence intensity in the presence and absence of the drug acting as quencher, respectively; K_{SV} and $[Q]$ are the Stern–Volmer quenching constant and concentration of the quencher (i.e., SXG or VDG), respectively. In Fig. 5 there are the plots of F/F^0 versus the $[Q]$ value of the drug at three investigated temperatures. As can be seen from Fig. 5 and the data listed in Table 1, a linear relationship between F/F^0 and the $[Q]$ values for SXG or VDG was obtained. The Stern–Volmer quenching constant values for the SXG-HSA and VDG-HSA complexes were calculated, and they were observed to decrease as the temperature increased. In order to distinguish the static quenching, the values for the quenching rate constant, k_q, were calculated *via* the following equation:

$$k_q = 1 + K_{SV}/\tau^0,$$

where τ^0 is the fluorophore lifetime in the absence of a quencher. Notably, the value of τ^0 for biomolecules is reported to be 10^{-8} s [23].The values calculated for k_q are listed in Table 1, and they were found to be 2.57×10^{12}, 2.05×10^{12}, and 1.45×10^{12} L/mol/s for SXG, and 4.73×10^{12}, 3.49×10^{12}, and 2.63×10^{12} L/mol/s for VDG at 298, 310, and 318 K, respectively .The obtained results indicate that the values for k_q were of the order of 10^{12} L/mol/s, which is higher than the maximum diffusion collision quenching rate constant (2.0×10^{10} M^{-1} s^{-1}) [24]. Therefore, HSA was assumed to undergo static quenching upon interaction with ei-

ther SXG or VDG [16]. Importantly, the decrease in the value of k_q in association with increases in the temperature provides additional proof that the complex formation takes place in consequence of an interaction between either of the two drugs and HSA.

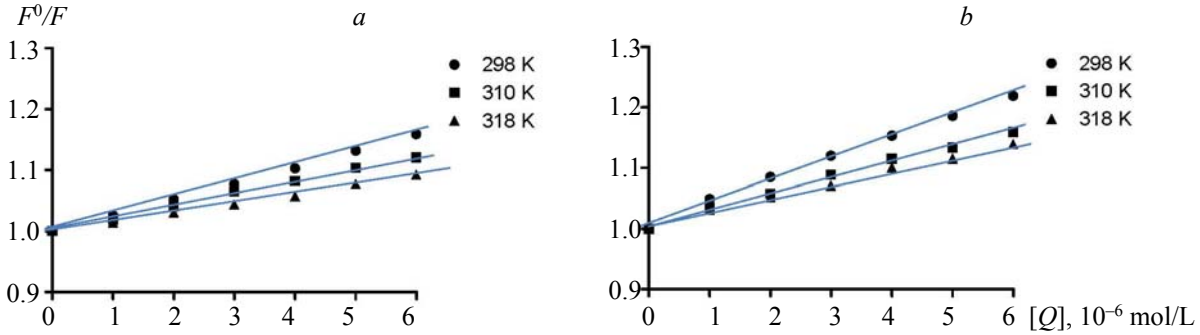

Fig. 5. a) Stern–Volmer plots for HSA-SXG system and b) Stern–Volmer plots for HSA-VDG system at temperatures 298, 310, and 318 K.

TABLE 1. The Parameters of Stern-Volmer Plots for the Quenching of HSA by SXG and VDG at Different Temperatures

Drug	T, K	K_{SV}, M^{-1}	K_q, M^{-1}/s^{-1}	R_1^2	n	K_a, M^{-1}	R_2^2
Saxagliptin	298	2.57×10^4	2.57×10^{12}	0.9966	1.034	4.003×10^4	0.9997
	310	2.05×10^4	2.05×10^{12}	0.9987	1.016	2.49×10^4	0.9980
	318	1.45×10^4	1.45×10^{12}	0.9977	1.039	2.42×10^4	0.9978
Vildagliptin	298	4.73×10^4	4.73×10^{12}	0.9967	0.902	1.13×10^4	0.9992
	310	3.49×10^4	3.49×10^{12}	0.9958	0.904	8.54×10^3	0.9942
	318	2.63×10^4	2.63×10^{12}	0.9961	0.903	7.15×10^3	0.9935

N o t e. K_{SV}: Stern–Volmer quenching constant; *n:* Number of binding sites; K_a: Binding constant obtained.

Determination of binding constant and number of binding sites. The HSA-drug binding constant (K_a) and the number of binding sites (n) were estimated employing the following equation [25]: $\log(F^0 - F)/F = \log K_a + n\log[Q]$. Plotting $\log[(F^0 - F)/F]$ versus $\log[Q]$ resulted in a straight line, whose slope equals n and whose intercept with the y-axis equals $\log K_a$ (Fig. 6). The calculated n value for the two HSA-drug complexes was about 1 in both cases, which suggests that there was a single binding site on HSA in the cases of both SXG and VDG. Thus, the calculated K_a values indicate a strong binding interaction between each of the two drugs and HSA. Notably, the K_a values were noticed to decrease as the temperature increased, which implies that the stability of the SXG-HSA and VDG-HSA complexes decreased at elevated temperatures.

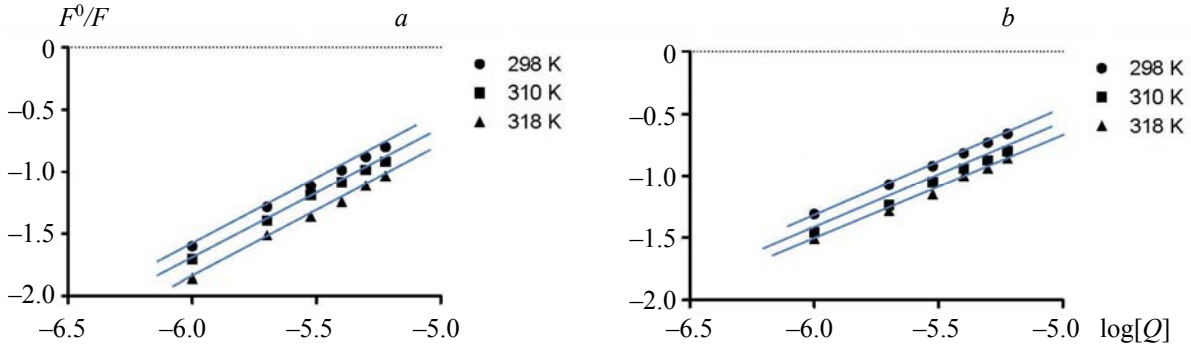

Fig. 6. The plot of $\log(F^0 - F)/F$ vs. $\log[Q]$ for quenching of HSA by (a) saxagliptin and (b) vildagliptin at 298, 310, and 314 K.

Calculation of thermodynamic parameters and investigation of binding forces. Noncovalent interactions (e.g., hydrogen bonding, van der Waals forces, electrostatic forces, and hydrophobic interactions) are known to play an important role in the stability of the complexes formed between serum albumin and drugs [26]. Hydrophobic interactions are mainly the motive force if ΔH and ΔS were positive values while van der Waals forces and hydrogen bonding forces are mainly present if obtained ΔH and ΔS were negative. Electrostatic forces are supposed to have a major role in the interaction when the ΔH value is negative and the ΔS are positive. In the present study, the ΔH and ΔS values for SXG-HSA and VDG-HSA complex formation were calculated via the following equation:

$$\ln K_a = -\Delta H/\mathrm{RT} + \Delta S/R.$$

Here, R is the gas constant and T is the temperature in the Kelvin scale.

The Gibbs free energy change (ΔG) could be calculated *via* the following equation [26, 27]:

$$\Delta G = \Delta H - - T\Delta S = -2.303\ \log K_a.$$

A plot of ln K_a versus $1/T$ was constructed at the three studied temperatures, and values for the relevant slopes and intercepts were used to calculate the binding reactions' ΔH and ΔS values, respectively (Table 2). The fact that the ΔG values were negative implies that the binding between each of the two drugs and HSA is spontaneous over the three studied temperatures [27]. Additionally, the positive values for ΔH, which remained constant as the values for K_a increased with the temperature, indicated that HSA-drug binding was an endothermic process. Moreover, the positive values for ΔS indicated that the binding was mainly entropy-driven. Based on the results just discussed, it is clear that hydrophobic forces have a predominant role in the binding interactions between HSA and the two drugs.

TABLE 2. Thermodynamic Parameters (Free Energy Change (ΔG), Enthalpy Change (ΔH), and Entropy Change (ΔS)) for HSA-SXG and HSA-VDG Mixtures at Different Temperatures

Drug	T, K	ΔG, kJ/mol	ΔH, kJ/mol	ΔS, J/mol/K
Saxagliptin	298	–26.256	25.02	216.1
	310	–26.091		
	318	–26.688		
Vildagliptin	298	–23.114	21.49	211.77
	310	–23.332		
	318	–23.464		

Molecular docking. Molecular docking provides a visual representation of how the drug may bind to HSA. The protein can bind a broad range of drugs, and much of the clinical and pharmaceutical interest in HSA arises from its effects on drug pharmacokinetics [28]. The MOE program was used to predict the possible conformations of SXG and VDG in the HSA-drug complexes. In these simulations, both SXG and VDG were found to bind through their side-chains containing the cyano group with the conservative amino acid Tyr161 in HSA (Fig. 7) at binding scores of −7.226 and −7.601 kcal/mol, at distances of 2.85 and 2.69 Å, respectively. Based on the previously mentioned experimental results, we can conclude that the results of the docking simulation afford a possible indication of the mode of binding of the two drugs to HSA.

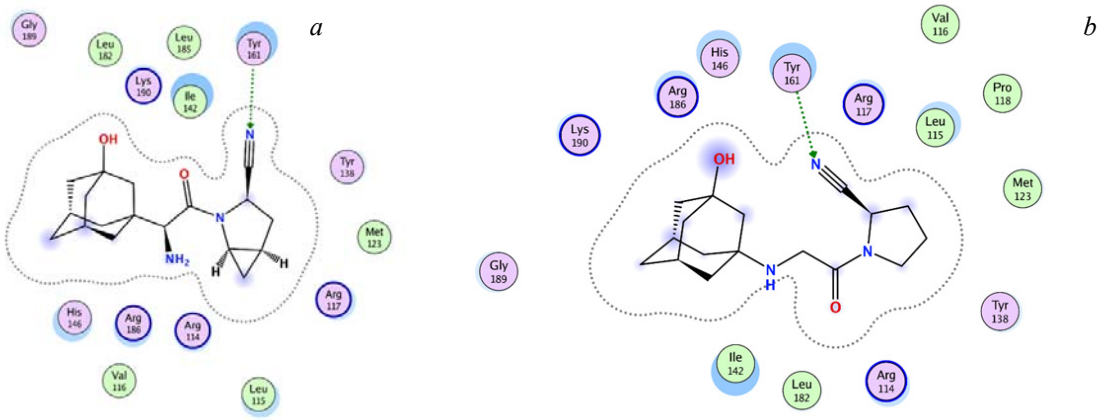

Fig. 7. Schematic view of the best configuration of the HSA-SXG (a) and HSA-VDG (b) complexes.

Despite being surrounded by many polar amino acids, the geometry of the most stable conformer identified in the docking study restricts the ligand exposure, which results in a distance larger than 3.5 Å between the polar groups of the drugs and the surrounding amino acids, which in turn prevents reliable hydrogen bond formation. The nature of the cyano group, which is linear due to the *sp*-hybridization of the carbon atom, makes it closer to the Tyr161 residue, making it possible for reliable interaction inside the pocket with the mentioned distances and energies [26].

FTIR spectroscopy. Infrared spectroscopy has been considered as an important approach to achieving the fast determination of the average secondary structure of proteins [29, 30]. The amide I is the most widely used one in studies of protein secondary structure from all the amides of the peptide group. This vibration mode is due to the C=O bond stretching vibration of the amide group, and it causes infrared bands to appear in the region between 1600 and 1700 cm^{-1} [29]. The change in HSA conformation after its binding to SXG or VDG can be investigated focusing on the FTIR band of amide I in HSA in the presence and absence of each drug. As can be seen from Fig. 8a, a strong FTIR absorption band at 1637 cm^{-1} attributable to amide I appears in the spectrum of native HSA, in the absence of SXG or VDG, which implies that HSA adopts mainly an α-helix-rich conformation. A slight change in the position and shape of the peak due to amide I is noticed after the addition of the drugs. Consequently, the interaction between HSA and SXG or VDG probably caused a rearrangement of the polypeptide carbonyl hydrogen bonding pattern due to SXG or VDG engaging in binding interactions with the C=O and N–H groups of the HSA (Fig. 8).

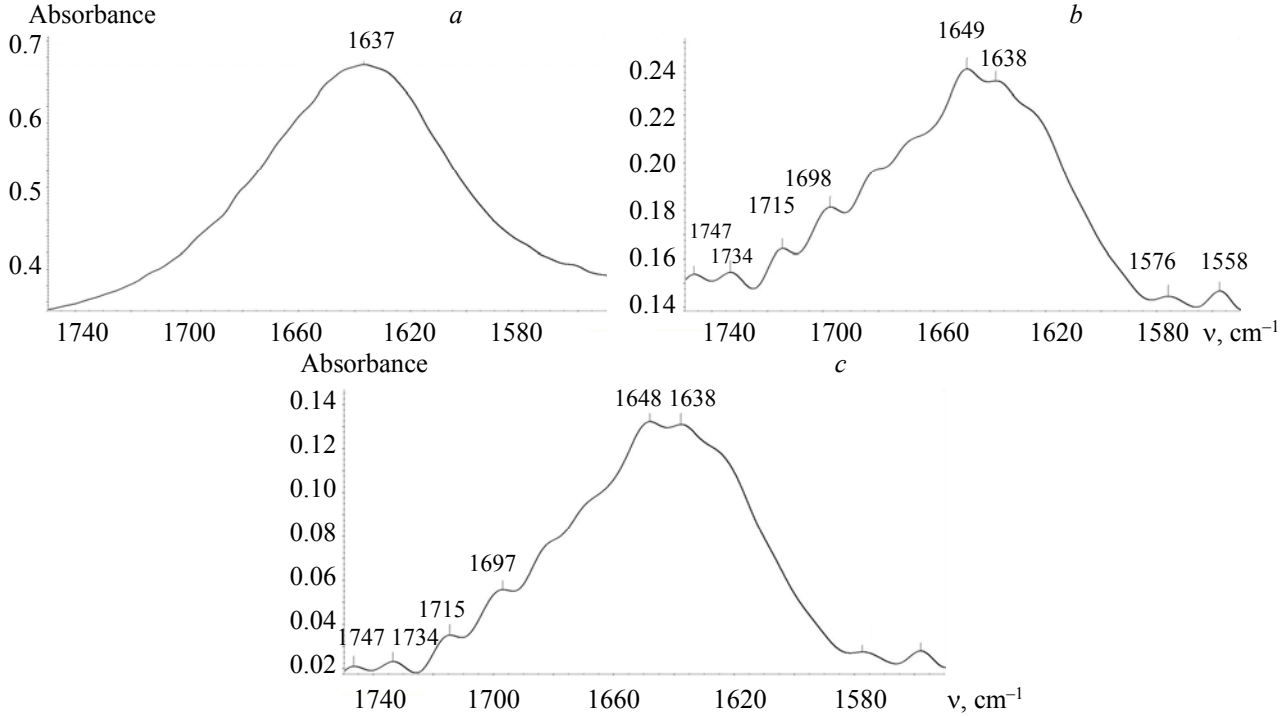

Fig. 8. FT-IR spectra of HSA. a) FT-IR spectra of free HSA; b) FT-IR spectra of HSA and saxagliptin c) FT-IR spectra of HSA and vildagliptin.

Competitive binding measurements using site markers. The competition for the binding sites of HSA between site-specific markers and both drugs was investigated implementing a simple technique. Specifically, IND, a typical marker for site I of HSA, and DIA, a typical marker for site II, were used to conduct displacement experiments. Fluorescence quenching data in the presence and absence of the said site markers were analyzed via the Stern–Volmer plots (Figs. 9). A data obtained suggest the competitive binding of site I and both drugs. The calculated values for K_{SV} are listed in Table 3. The calculated values for the binding constants indicate that the binding between SXG or VDG and HSA was suppressed in the presence of IND; by contrast, the presence of DIA had no effect on the value of the binding constant. Consequently, both drugs can be concluded to bind at or near site I of subdomain IIA of HSA. These results are in accordance with the results obtained from molecular docking simulations.

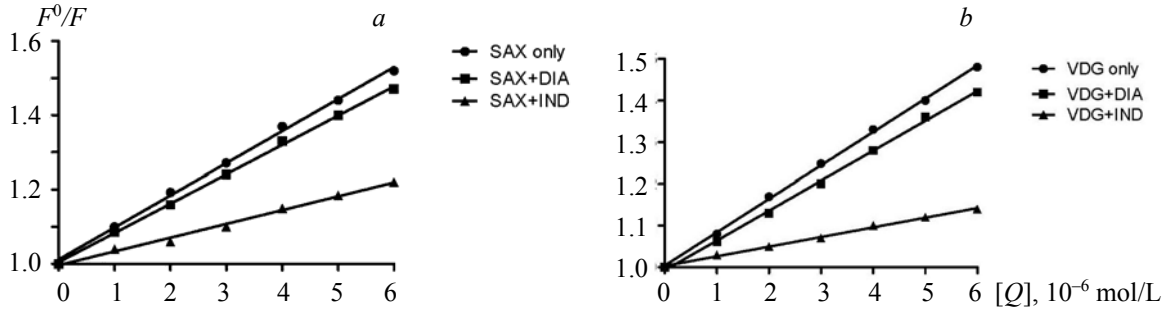

Fig. 9. a) Stern–Volmer plots for HSA-SXG (a) and HSA-VDG (b) system alone and in the presence of the site markers.

TABLE 3. Effect of Markers Ligands on K_{SV} for the Interaction of SXG and VDG with HSA at 298 K

Drug	Parameter	Drug only	With IND	With DIA
Saxagliptin	K_{SV}	2.67×10^5	3.6×10^4	8.02×10^4
	R^2	0.999	0.993	0.998
Vildagliptin	K_{SV}	8.17×10^4	2.5×10^4	6.7×10^4
	R^2	0.999	0.997	0.998

Conclusions. The interaction of HSA with the anti-diabetes drugs SXG and VDG was studied. The obtained results indicated that, as a consequence of the mentioned HSA–drug interactions, the intrinsic fluorescence of the protein was quenched *via* a static mechanism, since the value of the effective quenching constant (K_{SV}) was found to be inversely related with the reaction temperature, and the quenching rate constant (k_q) was observed to have values that were larger than 2.0×10^{10} M^{-1} s^{-1}, the maximum diffusion collision quenching rate constant. Additionally, the calculated thermodynamic parameters and the results of the molecular docking simulations for the binding interaction between HSA and each of the two drugs indicated that the main driving forces of the HSA-drug complex formation were hydrophobic, hydrogen bonding, and van der Waals ones. Evidence also suggested that the binding of SXG and VDG to HSA is an enthalpy-driven process. On the other hand, UV-Visible absorption and synchronous fluorescence data indicated that binding of either drug to HSA resulted in a slight change in the conformation of the protein. In general, the present study focused on investigating the nature of the interactions of SXG and VDG with HSA *in vitro* under simulated physiological conditions (pH 7.4), allowing further investigation on the pharmacological behavior of those drugs. This work can help provide important information on the transportation and storage of SXG and VDG in the human body, quite aside from these drugs' mode of action and pharmacokinetic properties.

REFERENCES

1. M. Lúcio, J. L. Lima, S. Reis, *Curr. Med. Chem*., **17**, No. 17, 1795–1809 (2010).
2. F. Hervé, S. Urien, E. Albengres, J. C. Duché, J. P. Tillement, *Clin. Pharm.*, **26**, No. 1, 44–58 (1994).
3. J. Koch-Weser, E. M. Sellers, *New Engl. J. Med*., **294**, No. 6, 311–316 (1976).
4. G. A. Ascoli, E. Domenici, C. Bertucci, *Chirality*, **18**, No. 9, 667–679 (2006).
5. S. C. Sweetman, *Martindale: The Complete Drug Reference. Drug Monographs*, Pharmaceutical Press, London (2011).
6. M. E. Cerf, *Front. Endocrinol. (Lausanne)*, **4**, 37 (2013).
7. S. E. Inzucchi, D. K. McGuire, *Circulation*, **117**, No. 4, 574–584 (2008).
8. A. R. Chacra, G. Tan, A. Apanovitch, S. Ravichandran, J. List, R. Chen, et al. *Int. J. Clin. Pract*., **63**, No. 9, 1395–1406 (2009).
9. L. N. Ji, C. Y. Pan, J. M. Lu, H. Li, Q. Li, Q. F. Li, et al. *Cardiovasc. Diabetol.*, **12**, No. 1, 118 (2013).
10. M. Takihata, A. Nakamura, K. Tajima, T. Inazumi, Y. Komatsu, H. Tamura, et al. *Diabetes Obes. Metab*., **15**, No. 5, 455–462 (2013).

11. C. Pan, X. J. T. Wang, *Ther. Clin. Risk Manag*., **9**, 247–257 (2013).
12. D. D. Zhang, N. Shi, H. Fang, L. Ma, W. P. Wu, Y. Z. Zhang, et al. *Exp. Ther. Med*., **15**, No. 6, 5100–5106 (2018).
13. Molecular Operating Environment (MOE) JSSW, suite 910, Montreal, QC, Canada, H3A 2R7. Chemical Computing Group ULC (2018).
14. K. Yamasaki, V. T. G. Chuang, T. Maruyama, M. Otagiri, *Biochim. Biophys. Acta*, **1830**, No. 12, 5435–5443 (2013).
15. F. L. Cui, J. Fan, J. P. Li, Z. D. Hu, *Bioorg. Med. Chem*., **12**, No. 1, 151–157 (2004).
16. J. Lakowicz, *Principles of Fluorescence Spectroscopy*, Springer Science & Business Media (2013).
17. T. S. Banipal, N. Kaur, P. K. Banipal, *J. Mol. Liq*., **223**, 1048–1055 (2016).
18. F. Hao, M. Jing, X. Zhao, R. Liu, *J. Photochem. Photobiol. B: Biol.*, **143**, 100–106 (2015).
19. B. Valeur, J.-C. Brochon, *New Trends in Fluorescence Spectroscopy: Applications to Chemical and Life Sciences*, Springer, Berlin (2012).
20. K. Shanmugaraj, S. Anandakumar, M. Ilanchelian, *Dyes Pigments*, **112**, 210–219 (2015).
21. H. Lin, J. Lan, M. Guan, F. Sheng, H. Zhang, *Spectrochim. Acta A: Mol. Biomol. Spectrosc.*, **73**, No. 5, 936–941 (2009).
22. M. Guo, W. J. Lü, M. H. Li, W. Wang, *Eur. J. Med. Chem*., **43**, No. 10, 2140–2148 (2008).
23. J. R. Lakowicz, G. Weber, *Biochemistry*, **12**, No. 21, 4161–4170 (1973).
24. W. R. Ware, *J. Phys. Chem*., **66**, No. 3, 455–458 (1962).
25. W. Xiaofang, L. Huizhou, *Chin. J. Anal. Chem.*, **28**, No. 6, 699–701 (2000).
26. J.-H. Shi, Y. Y. Zhu, J. Wang, J. Chen, Y. J. Shen, *Spectrochim. Acta A*: *Mol. Biomol. Spectrosc*., **103**, 287–294 (2013).
27. P. D. Ross, S. Subramanian, *Biochemistry*, **20**, No. 11, 3096–3102 (1981).
28. A. A. Bhattacharya, T. Grüne, S. Curry, *J. Mol. Biol.*, **303**, No. 5, 721–732 (2000).
29. A. Barth, *BBA-Bioenergetics*, **1767**, No. 9, 1073–1101 (2007).
30. Y. V. Il'ichev, J. L. Perry, *J. Phys. Chem. B*, **106**, No. 2, 452–459 (2002).